RSC Advances

PAPER

View Article Online
View Journal | View Issue

Cite this: *RSC Adv.*, 2016, **6**, 18711

Relay recognition of F^- and a nerve-agent mimic diethyl cyano-phosphonate in mixed aqueous media: discrimination of diethyl cyanophosphonate and diethyl chlorophosphate by cyclization induced fluorescence enhancement†

Avijit Kumar Das,[a] Shyamaprosad Goswami,*[a] Ching Kheng Quah[b] and Hoong-Kun Fun[bc]

Received 18th November 2015
Accepted 1st February 2016

DOI: 10.1039/c5ra24392k

www.rsc.org/advances

Anion to nerve agent simulant detection by relay recognition has been designed and realized for the first time with sequence specificity ($F^- \rightarrow$ DCNP) *via* a fluorescence "off–on–on" mechanism. The discrimination of DCNP and DCP *via* a CIFE (cyclization induced fluorescence enhancement) mechanism has also been demonstrated here. Test strips based on the sensors with F^- and DCNP are fabricated, which can act as convenient and efficient nerve agent and F^- test kits. The origin of the sequence specificity of different fluorescence recognition was revealed through single X-ray crystal and NMR analysis.

Introduction

Compared to the normal traditional chemosensor method (displacement of a metal complex by anions[1] and employment of an ion-pair receptor through cooperative interactions among co-bound ions and a heteroditopic host[2]) depending on the nature and reactivity of the chemodosimetric centres, an alternative chemodosimeter approach[3] based on an irreversible specific chemical reaction has emerged as an active research area of significant importance recently. But the bi-functional chemodosimetric centres, which refer to those based on a single host platform that give distinct colorimetric and fluorescence responses independently by recognizing two different guest species in the same or different channels, have gradually become a new and fantastic research focus in the field of fluorescence sensors specially by the chemodosimetric field.[4] On this occasion, we have employed a single chemosensor which selectively binds F^- and DCNP in a relay manner by a different chemical reaction based approach. As the smallest anion, F^- has unique chemical properties and it is widely used as an essential ingredient in toothpaste, pharmaceutical agent and even its addition to drinking water due to their tendency to prevent dental caries,[5] enamel demineralization and for the treatment of osteoporosis.[6] Based on the chemical affinity between silicon and fluoride, a variety of chemosensors has recently undergone a quiet revolution[7] and we have used this fluoride mediated de-silylation technique as the first step of the relay recognition phenomenon. On the other hand, nerve agents are among the most important and lethal classes of chemical-warfare agents (CWAs) and their use in terrorist attacks has led to increasing interest in the development of reliable and accurate methods to detect these lethal chemicals.[8] Among CW species, nerve agents are especially hazardous and can cause death within minutes after exposure and the United Nations classify them as weapons of mass destruction. Sarin, Soman and Tabun are by far the most known chemical warfare agents among the nerve gases in which the electrophilic centre is easily attacked by different functional groups. Depending on this specific chemical nature of these nerve gases and to overcome the limitations to the different biochemical and instrumental methods (biosensors,[9] ion mobility spectroscopy (IMS),[10] electrochemistry,[11] micro-cantilevers,[12] photonic crystals,[13] optical-fibre arrays[14]), an alternative way for the development of easy-to-use fluorogenic and chromogenic chemosensors for the detection of these gases have gained interest in recent years.[15] The nerve-gas-mimics diethyl cyanophosphonate (DCNP), diethyl chlorophosphate (DCP) and diisopropyl fluorophosphate (DFP) are normally used in such studies as they are the compounds that show the same reactivity as the real nerve agents, that is, Sarin, Soman and Tabun, but lack the severe toxicity.

[a]*Department of Chemistry, Indian Institute of Engineering Science and Technology, Shibpur, Howrah-711 103, India. E-mail: spgoswamical@yahoo.com; Fax: +91 33 2668 2916; +91 33 2668 2961-3*

[b]*X-ray Crystallography Unit, School of Physics, Universiti Sains Malaysia, 11800 USM, Penang, Malaysia*

[c]*Department of Pharmaceutical Chemistry, College of Pharmacy, King Saud, University, Riyadh 11451, Saudi Arabia*

† Electronic supplementary information (ESI) available: Experimental, spectroscopic details and crystallographic analysis. CCDC 1415425. For ESI and crystallographic data in CIF or other electronic format see DOI: 10.1039/c5ra24392k

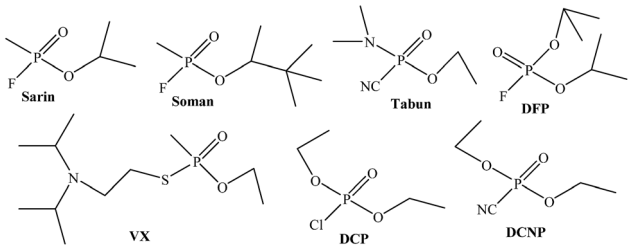

Fig. 1 The structures of nerve agents and their mimics.

The close reactivity is related with the presence of "similar" leaving groups (*i.e.* F, Cl and CN) in DFP, DCP and DCNP to those found in Sarin, Soman and Tabun (*i.e.* F and CN). Moreover DFP, DCP and DCNP are less toxic and in fact are not viable nerve agents because are readily hydrolysed (poorly persistent) when compared with Sarin, Soman and Tabun. Herein, we report a specific chemodosimeter molecule for the differentiation DCNP (tabun mimic) from other nerve agent mimics as well as the strong electrophiles. The main observable structural difference among DCNP (tabun mimic) and other nerve agents or their mimics is the electrophilic phosphorous centre is bonded to cyanide anion which is more reactive nucleophile to attack any nucleophilic centres. Whereas in case of other nerve agents, the anions other than cyanide like less reactive nucleophiles fluoride, thiolate and chloride were bonded to electrophilic phosphorous centre of the nerve agents (Fig. 1). Thus by targeting both the electrophilic character of phosphorus and nucleophilic character of cyanide anion present in tabun, we have designed and synthesized specific colorimetric and fluorometric probe for DCNP which is also less toxic than its mimic nerve gas tabun.

Results and discussions

Here we have proposed a relay recognition strategy in a single platform as a new pathway by using two analytes (F^- and DCNP) in a single fluorescent probe BSNA and here we disclose anion (F^-) to nerve gas relay recognition by using sequential chemodosimetric approaches which demonstrate significant improvement of fluorescence in different channel by fluoride induced desilylation followed by the use of iminocoumarin (as a DCNP signalling site) – benzothiazole in naphthol backbone.

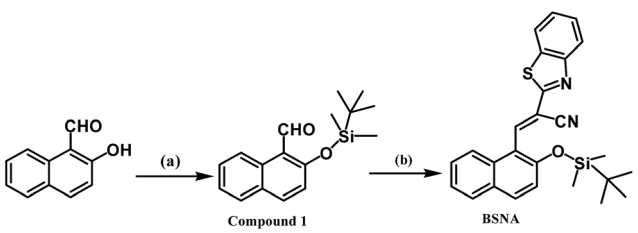

Scheme 1 Reagents and conditions: (a) *tert*-butyldimethylsilyl chloride, imidazole, dry DCM, 0 °C, 8 h, under N_2. (b) 2-Benzothiazole acetonitrile, 2–3 drops piperidine, dry EtOH, r.t.

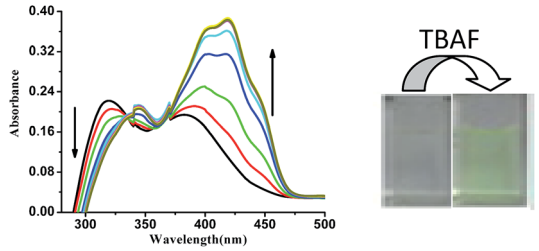

Fig. 2 UV-vis absorption spectra of **BSNA** in CH_3CN–H_2O (5/5, v/v) at pH 7.4 by using 10 mM HEPES buffer solution upon titration with 4.0 equiv. of TBAF. Inset: the naked eye color change of **BSNA** solution on addition of TBAF.

The intermediate silyl derivative (compound 1) was prepared by the silyl protection of hydroxyl group of 2-hydroxy-1-naphthaldehyde with *tert*-butyldimethylsilyl chloride (TBDMSCl) by using a catalytic amount of imidazole in dry CH_2Cl_2. The targeted compound **BSNA** [(*E*)-2-(benzothiazol-2-yl)-3-(2-(*tert*-butyldimethyl-silyloxy)naphthalene-1-yl) acrylonitrile] was prepared by the condensation reaction of compound 1 with 2-benzothiazole acetonitrile using two drops of piperidine in dry ethanol (Scheme 1).

To use **BSNA** as a chemosensor for the sequential sensing of F^- and DCNP in a relay manner, at first the selectivity of the sensor towards F^- is studied in CH_3CN : H_2O (v/v, 5 : 5) at pH 7.4 by UV-vis and fluorescence spectra. The UV-vis spectrum of **BSNA** shows moderately strong absorption band at 320 nm and 385 nm.

The absorption study of **BSNA** solution ($c = 2 \times 10^{-5}$ M) is carried out with F^- ion, the addition of gradually increasing concentrations of fluoride (as its tetrabutylammonium salt) resulted the decrease of the absorption peak at 320 nm and increase of the absorption peak at 410 nm with an isosbestic point at 335 nm in dramatic color development from colorless to pale green (Fig. 2).

The **BSNA** shows a weak emission band at 486 nm in acetonitrile/H_2O (5/5, v/v, 25 °C) at pH 7.4 by using 10 mM HEPES buffer solution in the absence of F^-. However, after addition of F^-, it immediately exhibits green fluorescence which results the increase of 12 fold emission intensity at the same wavelength (486 nm) through a specific cyclization reaction triggered by the strong affinity of fluoride toward silicon by the formation of

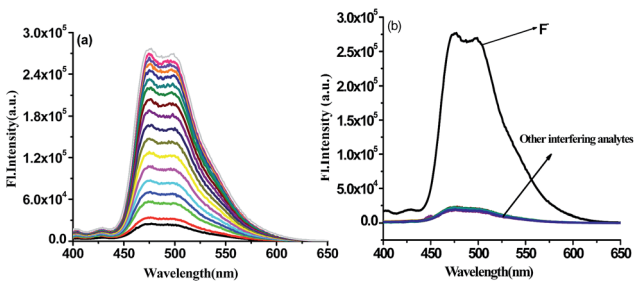

Fig. 3 (a) Fluorescence spectra of the receptor **BSNA** with TBAF in CH_3CN/H_2O (5/5, v/v, 25 °C) at pH 7.4 by using 10 mM HEPES buffer solution. (b) Change of emission intensity in **BSNA** after addition of each of the guest anions ($c = 2 \times 10^{-4}$ M).

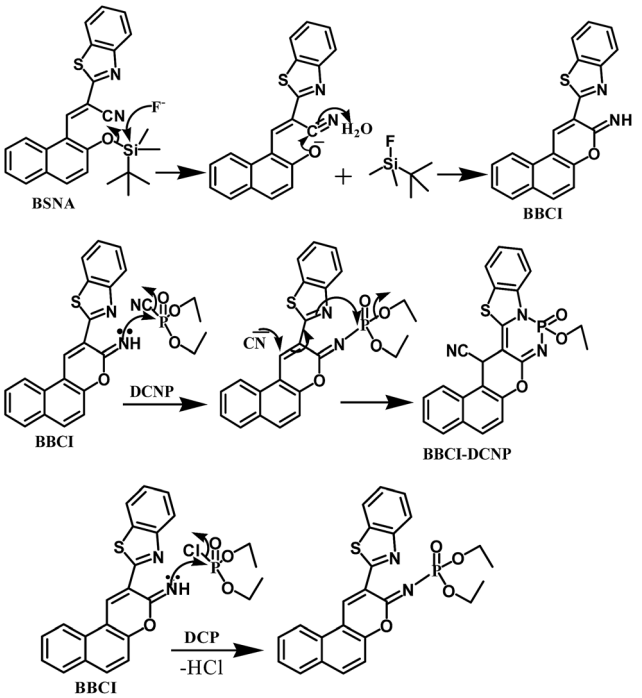

Scheme 2 The probable reaction mechanism of **BSNA** with F^- and **BBCI** with DCNP.

fluorescent compound **BBCI** [2-(benzothiazol-2-yl)-3*H*-benzochromen-3-imine] (Fig. 3, Scheme 2). But the addition of other analytes (such as Cl^-, Br^-, I^-, NO_3^-, NO_2^-, AcO^-, SCN^-, N_3^-, DHP, ATP, CN^-, HSO_4^-, SO_3^{2-}, DCP, DCNP) to **BSNA** solution does not show any response to break the oxygen–silyl bond and also to create any observable fluorescence (Fig. 3b). On the other hand, if we add DCNP to *in situ* system generated **BBCI** by the reaction of **BSNA** with F^-, a large increase of emission intensity (8 fold) occurs intensifying the emission color intensity by changing the green fluorescence to bluish white by the appearance of an emission peak at 480 nm (Scheme 3). The other analytes remain innocent to the *in situ* generated **BBCI** solution except DCP (Fig. 4).

The probable initial attack of the lone pair of imino nitrogen (assisted also by conjugated lone pair on oxygen of iminocoumarin) of **BBCI** takes place to DCNP releasing the CN^- ion which attacks the double bond of imino-coumarin moiety and the resulting ICT *via* resonance from imino-coumarin ring to benzothiazole nitrogen forms a six-membered cyclic product (**BBCI**–DCNP).

The cyclization induced fluorescence enhancement (CIFE) is also responsible for the generation of bluish-white fluorescence. In case of DCP the initial attack by the lone pairs of nitrogen of acidic –NH of **BBCI** to DCP creates slight fluorescence enhancement but due to the absence of any leaving nucleophilic group like CN^- in DCNP (released Cl^- from DCP is less nucleophilic rather than CN^- from DCNP), the probability of formation of cyclic product is almost nil which differs DCNP here from DCP by using our interesting chemodosimetric probe **BSNA** (Scheme 2). As indicated in the ^{1}H-NMR spectra, after

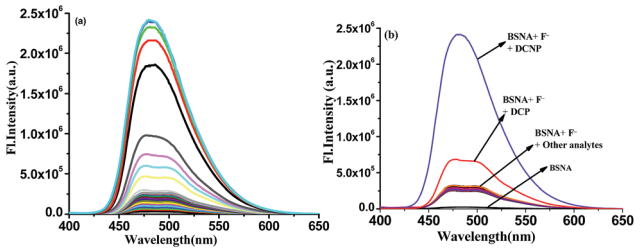

Fig. 4 (a) Fluorescence spectra of *in situ* system generated **BBCI** (**BSNA** + F^-) ($c = 2 \times 10^{-5}$ M) with DCNP in CH_3CN/H_2O (5/5, v/v, 25 °C) at pH 7.4 by using 10 mM HEPES buffer solution. (b) Fluorescence spectra of *in situ* generated **BBCI** (**BSNA** + F^-) with DCNP, DCP and other interfering analytes in CH_3CN/H_2O (5/5, v/v, 25 °C) at pH 7.4 by using 10 mM HEPES buffer solution ($c = 2 \times 10^{-4}$ M).

addition of DCP to the **BBCI** solution, the imino-coumarin proton signal vanishes for the formation of phosphoramide linkage and the proton signals arise at δ 3.2 ppm and δ 1.4 ppm for $-CH_2-$ and $-CH_3-$ group respectively (Fig. S5†).

The addition of DCNP to the solution of **BBCI** solution does not change significantly in the absorption spectra of the solution (Fig. 5a). The fluoride induced de-silylated fluorescent cyclic product **BBCI** is also isolated, purified and characterized by single X-ray crystal study. The fluorescence spectra of **BBCI** and the increase of its emission intensity by addition of DCNP is also identical with the *in situ* generated **BBCI** (Fig. 5b) and the silyl bonded fluoride ion does not interfere the sensing of DCNP by *in situ* **BBCI.**

It is revealed that the green fluorescence of **BSNA** solution can be detected by using minimum 2.84 μM of F^- in fluorescence spectra and 3.09 μM of DCNP detects the bluish white fluorescence of **BBCI** solution (Fig. S1†). The fluoride induced de-silylation rate constant of **BSNA** (K) = 2.01×10^{-2} s^{-1} and the changes of emission at different time intervals by addition of DCNP to the **BBCI** solution, at fixed wavelength at 480 nm by using first order rate equation, the rate constant (K) is found to be 1.4×10^{-2} s^{-1}. The probe **BSNA** itself exhibited negligible fluorescence corresponding to a peak of weak emission intensity at 486 nm on excitation at 380 nm having low fluorescence quantum yield ($\Phi = 0.001$). The quantum yield of new emission band at 486 nm was 0.158 (increase of 158 fold) upon addition of F^- to the **BSNA** solution and 0.256 for DCNP to the **BBCI**

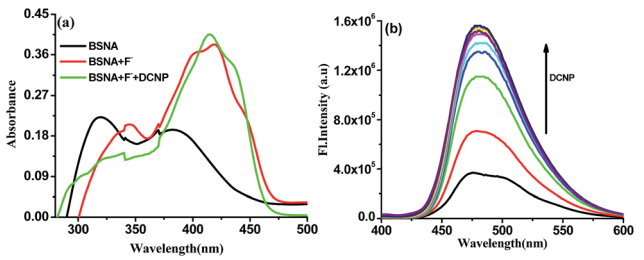

Fig. 5 (a) Comparison of absorption spectra of **BSNA**, **BBCI** and **BBCI** + DCNP in CH_3CN/H_2O (5/5, v/v, 25 °C) at pH 7.4 by using 10 mM HEPES buffer solution. (b) Fluorescence spectra of isolated de-silylation product of **BSNA** with TBAF (**BBCI**) with DCNP in CH_3CN/H_2O (5/5, v/v, 25 °C) at pH 7.4 by using 10 mM HEPES buffer solution.

Fig. 6 Upper panel: The fluorescence changes in the solid phase. Lower panel: The naked eye color change in the ambient light in the solid phase.

solution corresponding to blue-shifted emission peak at 480 nm (increase of 256 fold). For the handy application of the sensing, dip-stick method is very much useful. In this method, the emission color change in the test strips was identified by immersing the TLC plate to the **BSNA**, **BBCI** and **BBCI** + DCNP solutions followed by evaporating the solvent to dryness. The emission and naked eye color change were observed on the plate from colorless to different colors (Fig. 6).

This type of dipstick method is very much helpful for the instant qualitative information without remedying any type of time consuming instrumental analysis. The competition experiment was also carried out by adding fluoride and DCNP to the solution of **BSNA** and **BBCI** respectively in the presence of commonly employed interfering analytes.

The selectivity profile diagram (Fig. 7) reveals that fluoride induced fluorescence enhancement remains almost unperturbed by the coexistence of other interfering analytes which remain innocent toward sensing of fluoride. The DCNP induced fluorescence enhancement also remains undisturbed in presence of different analytes except slight interference by DCP.

In the comparison of ^{1}H-NMR spectra (Fig. 8; Scheme 3), we have seen that the H_a proton of **BSNA** shows a sharp peak at δ 8.71 ppm. But after addition of TBAF to BSNA solution the fluoride induced desilylation renders to the formation of imino-

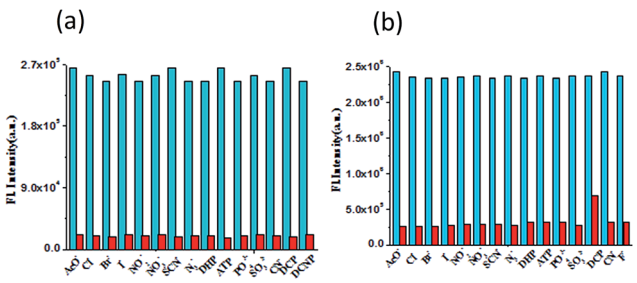

Fig. 7 Fluoride and DCNP selectivity profile of the sensor **BSNA** and **BBCI** respectively: (a) (red bars) change of fluorescence of BSNA + 10.0 equiv. of different analytes; (turquoise bars) change of fluorescence of sensor + 10.0 equiv. of different analytes, followed by 10.0 equiv. F^- at 486 nm. (b) (red bars) Change of emission intensity of BBCI + 10.0 equiv. of different analytes; (turquoise bars) change of emission intensity of sensor + 8.0 equiv. of different analytes, followed by 8.0 equiv. DCNP at 480 nm.

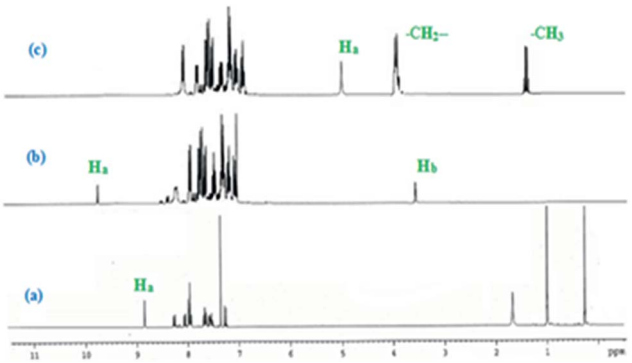

Fig. 8 Comparison of partial ^{1}H-NMR spectra of (a) **BSNA**; (b) **BBCI**; (c) **BBCI** + DCNP in $CDCl_3$.

coumarin moiety (**BBCI**) in which the Ha proton shifted to higher region at δ 9.77 ppm due to deshielding effect by the strong electron withdrawing effect of cyanide and benzothiazole ring and a new peak appears at δ 3.75 ppm corresponding to –NH proton signal (Hb). On addition of DCNP to **BBCI** solution, due to high acidic property of –NH proton, it attacks DCNP to make free cyanide ion which further attacks the double bond of imino coumarin moiety which results diminishing of –NH proton signal and the shifting of Ha proton in higher field at δ 5.37 ppm due to cyanide attack.

The reaction of **BBCI** with DCNP was also examined by the treatment of **BBCI** with DCNP and subjecting the reaction solution to ESI-MS analysis. The ^{1}H-NMR spectra (Fig. S10†) and a major peak located at 445.0569 was identified (Fig. S11†), which is consistent with the theoretical exact mass of the **BBCI**–DCNP complex ($C_{23}H_{16}N_3O_3PS^+$; 445.065), confirming the formation of the compound in the assay system. Thus by the ^{1}H-NMR, HRMS and X-ray crystallography, the probable mechanism for the sensing of F^- and DCNP in a single platform (**BSNA**) in a relay manner can be explained (Scheme 3).

The silyl-protected **BSNA** at first reacts with fluoride and fluoride induced desilylation of the –OTBDMS group of **BSNA** forms a fluorescent compound iminocoumarin in naphthol backbone which is responsible for the generation of green fluorescence at 486 nm. Then after addition of DCNP to the **BSNA** + F^- solution, the reactive imino nitrogen reacts with DCNP to release CN^- which reacts with the double bond of iminocoumarin ring (**BBCI**) to form the cyclic product (**BBCI**–DCNP) and increases the fluorescence at 480 nm (green fluorescence turns to slight bluish white) (Scheme 3).

Scheme 3 Anion to nerve gas relay in iminocoumarin benzothiazole platform in 2-hydroxy-1-naphthaldehyde backbone by "off–on–on" phenomenon.

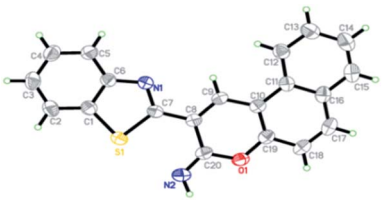

Fig. 9 The molecular structure of the **BBCI**, showing 50% probability displacement ellipsoids for non-H atoms and the atom-numbering scheme.

In the X-ray crystallographic studies of **BBCI** (Fig. 9), the 3*H*-benzo[*f*]chromene ring system, is almost planar, with a r.m.s. deviation of 0.067 Å, and makes a dihedral angle of 7.60(6)° with the benzo[*d*]thiazole ring system. In the crystal, no intermolecular hydrogen bonds are observed. The molecules are stacked along the *a*-axis and are consolidated by weak π–π interactions involving the thiazole/benzene (C10/C11/C16–C19) and thiazole/2*H*-pyran rings [centroid–centroid distances of 3.6641(13) and 3.6849(12) Å, respectively].

Conclusion

In conclusion here an unprecedented relay recognition of anion F^- and nerve agent simulant DCNP has been achieved and further demonstrated for the selectivity of DCNP over DCP by colorimetric and fluorimetric pathway. The *in situ* system generated **BBCI** from the sensing of F^- to the system **BSNA** and also the isolated product **BBCI** showed good relay recognition ability for DCNP *via* the formation of a six-member cyclic product (**BBCI**–DCNP) which is also responsible for the generation of fluorescence in different channel. For practical application, the dipstick method by using different test strips on the sensors is very much helpful for the instant qualitative information without remedying any type of time consuming instrumental analysis for the detection of F^- as well as DCNP.

General

Unless otherwise mentioned, chemicals and solvents were purchased from Sigma-Aldrich chemicals Private Limited and were used without further purification. Melting points were determined on a hot-plate melting point apparatus in an open-mouth capillary and are uncorrected. ^{1}H-NMR spectra were recorded on Brucker 300 MHz instrument. For NMR spectra, $CDCl_3$ was used as solvent using TMS as an internal standard. Chemical shifts are expressed in δ units and ^{1}H-^{1}H and ^{1}H-C coupling constants in Hz. UV-vis titration experiments were performed on a JASCO UV-V530 spectrophotometer and fluorescence experiment was done using PerkinElmer LS 55 fluorescence spectrophotometer using a fluorescence cell of 10 mm path.

General method of UV-vis and fluorescence titration

By UV-vis method. For UV-vis titrations, stock solution of the sensor was prepared ($c = 2 \times 10^{-5}$ M) in was studied in $CH_3CN : H_2O$ (v/v, 5 : 5) at pH-7.4 by using 10 mM HEPES buffer solution. Solutions of various concentrations containing sensor and increasing concentrations of different analytes were prepared separately. The spectra of these solutions were recorded by means of UV-vis methods.

By fluorescence method. For fluorescence titrations, stock solution of the sensor ($c = 2 \times 10^{-5}$ M) was prepared for the titration of different analytes in $CH_3CN : H_2O$ (v/v, 5 : 5) at pH-7.4 by using 10 mM HEPES buffer solution. The solution of the different guests like F^-, Cl^-, Br^-, I^-, NO_3^-, NO_2^-, AcO^-, SCN^-, N_3^-, DHP, ATP, CN^-, HSO_4^-, SO_3^{2-}, DCP, DCNP were also prepared in the order of ($c = 2 \times 10^{-4}$ M). Solutions of various concentrations containing sensor and increasing concentrations of different ions were prepared separately. The spectra of these solutions were recorded by means of fluorescence methods.

Determination of fluorescence quantum yield. Here, the quantum yield ϕ was measured by using the following equation,

$$\phi_x = \phi_s(F_x/F_s)(A_s/A_x)(n_x^2/n_s^2)$$

where, x & s indicate the unknown and standard solution respectively, ϕ = quantum yield, F = area under the emission curve, A = absorbance at the excitation wave length, n = index of refraction of the solvent. Here ϕ measurements were performed using anthracene in ethanol as standard [$\phi = 0.27$] (error ~10%).

Experimental

Synthesis of 2-hydroxy-1-napthylaldehyde

2-Hydroxy-1-napthylaldehyde was synthesized by the reported procedure.[16] β-Naphthol (1 g, 0.0069 mol) was placed in a 100 mL r.b. flask fitted with a reflux condenser, a magnetic stirrer and a dropping funnel. It was then dissolved in EtOH at 80–90 °C. NaOH (2 g, 0.05 mol) in 20 mL water was then added dropwise to this hot solution when the solution became darker. After half an hour, $CHCl_3$ (1.3 g, 0.011 mol) was added dropwise using a dropping funnel. Development of deep blue coloration indicates the reaction has started. Near the end point of the addition, the sodium salt of the phenolic aldehyde was separated out. The reaction mixture was stirred for six hours. Excess ethanol and chloroform were distilled off. The dark oil left was mixed with a considerable amount of sodium chloride. Sufficient water was added to dissolve the salt, and the oil was separated and washed with hot water. Then, the solution was neutralized with dilute hydrochloric acid and extracted with chloroform. Finally, the product was purified by 60–120 silica gel by 1–2% ethyl acetate in pet ether. Yield of the product was 500 mg (50%). Melting point: 79–80 °C.

Synthesis of BSNA

2-Hydroxy-1-napthylaldehyde (300 mg, 1.74 mmol) was dissolved in dry dichloromethane under nitrogen atmosphere at 0 °C. Than catalytic amount imidazole (70 mg, 1.02 mmol) was added to it and stirred for half an hour. Tetrabutyl dimethyl silyl chloride (262 mg, 1.74 mmol) was added slowly to the reaction

mixture and a white precipitation is separated out. The whole mixture was stirred at room temperature for 3 h. After completion of the reaction, water was added and the compound was extracted with dichloromethane. The volume of organic solvent was reduced under high pressure and the crude gummy product (compound 1) was directly used to the next step without purification by column chromatography due to its high instability. The compound 1 was dissolved in dry ethanol under nitrogen atmosphere. After stirring for few minutes, 2-benzothiazole acetonitrile (200 mg, 1.15 mmol) and 2–3 drops piperidine were added to the reaction mixture. After completion the reaction monitored by TLC, the target product BSNA was purified by column chromatography using 10% ethyl acetate in pet ether (v/v). Yield-500 mg, 65%.

Mp. 120–130 °C.

^{1}H NMR ($CDCl_3$, 300 MHz): δ (ppm): 8.71 (s, 1H), 8.11 (m, 1H), 7.95 (m, 1H), 7.92 (m, 1H), 7.83 (d, 2H, $J = 1.2$ Hz), 7.67 (d, 2H, $J = 7.8$ Hz), 7.56 (m, 1H), 7.41 (m, 1H), 7.14 (d, 1H, $J = 6.3$ Hz), 1.65 (s, 3H), 1.02 (s, 9H), 0.26 (s, 3H).

HRMS (ESI-TOF): (*m*/*z*, %): M + calculated for $C_{26}H_{26}N_2OSSi$ is 442.1535; found: 443.1609 $(M + H)^+$; $(M + Na)^+$ calculated 465.1433; found: 465.1389.

Elemental analysis: calculated value: C, 70.55; H, 5.92; N, 6.33; observed value: C, 70.51; H, 5.94; N, 6.35.

Synthesis of BBCI

To a stirred solution of **BSNA** (300 mg, 0.68 mmol) in CH_3CN (10 mL) was added tetrabutylammonium fluoride (180 mg, 0.68 mmol) at room temperature. The mixture was stirred for 3 h, and the solvent was evaporated under reduced pressure. The resulting crude residue was purified by flash column chromatography (10 : 1 → 1 : 1) on silica gel to afford BBCI as an orange solid (150 mg, 67%).

Mp. 220–230 °C.

^{1}H NMR ($CDCl_3$, 300 MHz): δ (ppm): 9.78 (s, 1H), 8.36 (d, 1H, J = 7.5 Hz), 8.13 (d, 1H, J = 3.9 Hz), 8.04 (m, 2H), 7.83 (d, 2H, J = 8.1 Hz), 7.77 (m, 1H), 7.65 (m, 1H), 7.54 (m, 1H), 7.48 (m, 1H), 3.76 (s, 1H).

HRMS (ESI-TOF): (*m*/*z*, %): M + calculated for $C_{20}H_{12}N_2OS$ is 328.067; found: 329.0745 $(M + H)^+$.

Elemental analysis: calculated value: C, 73.15; H, 3.68; N, 8.53; observed value: C, 74.18; H, 3.66; N, 8.52.

Acknowledgements

Authors thank the DST and CSIR (Govt. of India) for financial support. A. K. D. acknowledges the CSIR for providing fellowships.

References

1 (*a*) B. T. Nguyen and E. V. Anslyn, *Coord. Chem. Rev.*, 2006, **250**, 3118; (*b*) S.-Y. Chung, S. W. Nam, J. Lim, S. Park and J. Yoon, *Chem. Commun.*, 2009, 2866; (*c*) S. Rochat and K. Severin, *Chem. Commun.*, 2011, **47**, 4391; (*d*) X. Su, T. F. Robbins and I. Aprahamian, *Angew. Chem., Int. Ed.*, 2011, **50**, 1841.

2 (*a*) S. K. Kim and J. L. Sessler, *Chem. Soc. Rev.*, 2010, **39**, 3784; (*b*) G. Reeske, G. Bradtm€oller, M. Sch€urmann and K. Jurkschat, *Chem.–Eur. J.*, 2007, **13**, 10239; (*c*) J. L. Sessler, S. K. Kim, D. E. Gross, C. H. Lee, J. S. Kim and V. M. Lynch, *J. Am. Chem. Soc.*, 2008, **130**, 13162; (*d*) Y. Chen, D. X. Wang, Z. T. Huang and M. X. Wang, *Chem. Commun.*, 2011, **47**, 8112.

3 (*a*) D. G. Cho and J. L. Sessler, *Chem. Soc. Rev.*, 2009, **38**, 1647; (*b*) D. T. Quang and J. S. Kim, *Chem. Rev.*, 2010, **110**, 6280; (*c*) M. E. Jun, B. Roy and K. H. Ahn, *Chem. Commun.*, 2011, **47**, 7583.

4 (*a*) L. Yuan, W. Lin, Y. Xie, B. Chen and S. Zhu, *J. Am. Chem. Soc.*, 2012, **134**, 1305; (*b*) R. Satapathy, Y. H. Wu and H. C. Lin, *Org. Lett.*, 2012, **14**, 2564; (*c*) R. Guliyev, S. Ozturk, E. Sahin and E. U. Akkaya, *Org. Lett.*, 2012, **14**, 1528; (*d*) M. Schmittel and S. Qinghai, *Chem. Commun.*, 2012, **48**, 2707.

5 (*a*) K. L. Kirk, *Biochemistry of the Halogens and Inorganic Halides*, Plenum Press, New York, 1991, p. 58; (*b*) H. S. J. Horowitz, *Public Health Dent*, 2003, **63**, 3–8.

6 (*a*) B. L. Riggs, *Bone and Mineral Research, Annual 2*, Elsevier, Amsterdam, 1984, pp. 366–393; (*b*) J. R. Farley, J. E. Wergedal and D. J. Baylink, *Science*, 1983, **222**, 330–332; (*c*) M. Kleerekoper, *Endocrinol. Metab. Clin. North Am.*, 1998, **27**, 441–452.

7 (*a*) R. Hu, J. Feng, D. Hu, S. Wang, S. Li, Y. Li and G. Yang, *Angew. Chem., Int. Ed.*, 2010, **49**, 4915–4918; (*b*) S. Y. Kim and J. I. Hong, *Org. Lett.*, 2007, **9**, 3109–3112; (*c*) O. A. Bozdemir, F. Sozmen, O. Buyukcakir, R. Guliyev, Y. Cakmak and E. U. Akkaya, *Org. Lett.*, 2010, **12**, 1400–1403; (*d*) S. Goswami, A. K. Das, A. Manna, A. K. Maity, H. K. Fun, C. K. Quah and P. Saha, *Tetrahedron Lett.*, 2014, **55**, 2633.

8 (*a*) J. J. Gooding, *Anal. Chim. Acta*, 2006, **559**, 137; (*b*) L. M. Eubanks, T. J. Dickerson and K. D. Janda, *Chem. Soc. Rev.*, 2007, **36**, 458; (*c*) B. M. Smith, *Chem. Soc. Rev.*, 2008, **37**, 470; (*d*) M. Wheelis, *Pure Appl. Chem.*, 2002, **74**, 2247; (*e*) H. H. Hill Jr and S. J. Martin, *Pure Appl. Chem.*, 2002, **74**, 2281; (*f*) S. Goswami, A. Manna and S. Paul, *RSC Adv.*, 2014, **4**, 21984; (*g*) A. K. Mahapatra, K. Maiti, S. K. Manna, R. Maji, S. Mondal, C. D. Mukhopadhyay, P. Sahoo and D. Mandal, *Chem. Commun.*, 2015, **51**, 9729–9732; (*h*) S. Goswami, S. Das and K. Aich, *RSC Adv.*, 2015, **5**, 28996.

9 (*a*) M. T. McBride, S. Gammon, M. Pitesky, T. W. O. Brien, T. Smith, J. Aldrich, R. G. Langlois, B. Colston and K. S. Venkateswaran, *Anal. Chem.*, 2003, **75**, 1924; (*b*) A. J. Russell, J. A. Berberich, G. F. Drevon and R. R. Koepsel, *Annu. Rev. Biomed. Eng.*, 2003, **5**, 1; (*c*) H. Wang, J. Wang, D. Choi, Z. Tang, H. Wu and Y. Lin, *Biosens. Bioelectron.*, 2009, **24**, 2377.

10 E. Steiner, S. J. Klopsch, W. A. English, B. H. Clowers and H. H. Hill, *Anal. Chem.*, 2005, **77**, 4792.

11 (*a*) M. A. K. Khan, Y. T. Long, G. Schatte and H. B. Kraatz, *Anal. Chem.*, 2007, **79**, 2877; (*b*) O. V. Shulga and C. Palmer, *Anal. Bioanal. Chem.*, 2006, **385**, 1116; (*c*)

J. C. Chen, J. L. Shih, C. H. Liu, M. Y. Kuo and J. M. Zen, *Anal. Chem.*, 2006, **78**, 3752.

12 G. Zuo, X. Li, P. Li, T. Yang, Y. Wang, Z. Chen and S. Feng, *Anal. Chim. Acta*, 2006, **580**, 123.

13 (*a*) W. He, Z. Liu, X. Du, Y. Jiang and D. Xiao, *Talanta*, 2008, **76**, 698; (*b*) J. P. Walker, K. W. Kimble and S. A. Asher, *Anal. Bioanal. Chem.*, 2007, **389**, 2115; (*c*) J. P. Walker and S. A. Asher, *Anal. Chem.*, 2005, **77**, 1596.

14 M. J. Aernecke and D. R. Walt, *Sens. Actuators, B*, 2009, **142**, 464.

15 (*a*) M. Burnworth, S. J. Rowan and C. Weder, *Chem.–Eur. J.*, 2007, **13**, 7828; (*b*) N. A. Rakow, A. Sen, M. C. Janzen, J. B. Ponder and K. S. Suslick, *Angew. Chem.*, 2005, **117**, 4604; *Angew. Chem., Int. Ed.*, 2005, **44**, 4528; (*c*) A. M. Costero, S. Gil, M. Parra, P. M. E. Mancini, R. Martinez- MaÇez, F. Sancenon and S. Royo, *Chem. Commun.*, 2008, 6002; (*d*) T. J. Dale and J. Rebek, *Angew. Chem.*, 2009, **121**, 7990; *Angew. Chem., Int. Ed.*, 2009, **48**, 7850.

16 (*a*) Fosse, *Bull. Soc. Chim. Fr.*, 1901, **25**, 373; (*b*) Kolesnikov, Korshak and Krakovnaya, *Zh. Obshch. Khim.*, 1951, **21**, 397.